The case for improving the Robinson formulas

Michael W. Liemohn[1]

[1] Department of Climate and Space Sciences and Engineering, University of Michigan, Ann Arbor, MI.

Corresponding author: Mike Liemohn (liemohn@umich.edu)

Key Points:

- The development and usage of the famous Robinson formulas, relating auroral precipitation to ionospheric conductance, is recounted
- Recent approaches to address shortcomings of these formulas are reviewed and discussed, noting shortcomings in some of these studies
- The space physics research community is urged to take on the action of improving the connection between precipitation and conductance

AGU Index Terms:

- 2407 Auroral ionosphere
- 2455 Particle precipitation
- 2764 Plasma sheet
- 2753 Numerical modeling
- 2704 Auroral phenomena

Keywords:

Aurora, electron precipitation, call to action, numerical modeling, ionospheric conductance

Abstract

Auroral particle precipitation is the main source of ionization on the nightside, making it a critical factor in geospace physics. This magnetosphere-ionosphere linkage directly contributes to, even controls, the nonlinear feedback within this coupled system. One study has dominated our understanding of this connection, presenting a pair of equations relating auroral particle precipitation to ionospheric Pedersen and Hall conductance, the famous Robinson formulas. This Commentary examines the history of the development and usage of the Robinson formulas and the recent studies exploring corrections and expansions to it. The conclusion is that more work needs to be done; the space physics research community should take up the task to develop improvements and enhancements to better quantify the connection of auroral precipitation to ionospheric conductance.

1. Introduction

Electron precipitation into the upper atmosphere ionizes the neutrals and enhances electric conductivity in the auroral zone. This conductivity, or more specifically its height-integrated version, conductance, is critical to the closure of field-aligned currents by horizontal Pedersen currents in the ionosphere. Over the decades, relationships between downflowing electron fluxes and ionospheric conductance have been derived, most notably by Robinson et al. (1987). This study has been widely used across space physics, garnering over 400 citations according to Google Scholar and roughly 300 according to CrossRef, yielding a dominant influence on our understanding of the precipitation-conductance relationship.

One aspect of the Robinson et al. (1987) study that makes it so ubiquitously adopted is its simplicity, relating the ionospheric Pedersen and Hall conductances, Σ_P and Σ_H, respectively, to two values of the downflowing electrons, called herein the Robinson formulas:

$$\Sigma_P = \frac{40\bar{E}}{16 + \bar{E}^2}\Phi_E^{1/2} \quad (1)$$

$$\frac{\Sigma_H}{\Sigma_P} = 0.45\bar{E}^{0.85} \quad (2)$$

Here, Φ_E is the energy flux of the downward precipitating electrons and $\bar{E}$ is the average energy of those precipitating electrons. These are straightforward to include in data analysis and modeling studies, allowing an easy relationship that helps advance our understanding of the geospace system.

There are some key studies among those that have adopted the Robinson formulas. For instance, Fedder et al. (1995) was the first usage of the Robinson formulas in a global magnetohydrodynamic (MHD) model. Using the plasma moments from MHD at the inner boundary of that code's simulation domain, the Robinson formulas, along with a discrete auroral

correction due to field-aligned potential drops between the inner MHD simulation boundary and the ionosphere, were used to obtain a two-dimensional distribution of conductance. This allowed for Ohm's law to be used to calculate the ionospheric electric potential, which was mapped to the inner boundary of the MHD domain and used to set perpendicular velocity there. This causal connection between the magnetosphere and ionosphere is critical for understanding the nonlinear feedback within the geospace system. One famous usage of this code for physical insight is the Brambles et al. (2011) study obtaining periodic tail reconfigurations resembling sawtooth oscillations, a feature that could not be reproduced by the MHD model without causally related conductance and outflow settings.

Other MHD calculations adopted a different approach. For example, Ridley et al. (2004) used a month of output from the assimilative mapping of ionospheric electrodynamics (AMIE) model to relate field-aligned currents (FACs) to ionospheric Pedersen and Hall conductance. The Robinson formulas were included in this model to convert these conductances to electron precipitation values for use in ionosphere-thermosphere models connected to this ionospheric potential solver. This relationship was applied to the kinetic drift physics model of Liemohn et al. (2005), showing plasmapause differences of up to 2 Earth radii and factors of several in the hot ion flux between the conductance settings.

The initial uses of the Robinson formulas with global models assumed that the MHD plasma parameters directly related to the precipitating electron characteristics. Several corrections to this have been applied in recent years. One of these is the work of Zhang et al. (2015), who updated the electron precipitation model for conductance from the Fedder et al. (1995) usage. Similarly, the Ridley et al. (2004) conductances were updated using plasma parameters and calculated electron distributions in this model by Yu et al. (2016). Perlongo et al. (2017), Chen et al. (2019), and Khazanov et al. (2019) each adopted the Robinson formulas with the electron precipitation calculations in their kinetic drift physics models. A recent summary of the magnetosphere-ionosphere coupling relationship and the conductance settings in various numerical models can be found in the review by Wiltberger et al. (2017), noting the overwhelming dominance of the Robinson formulas in such codes.

For all of its benefits to the field of space physics, the Robinson formulas have issues. This report details those issues and puts forward a call to action for the research community to develop a new and more robust version of the Robinson formulas.

2. History of the Robinson formulas

To understand the limitations of the Robinson conductance formulas, it is useful to explore the history of their development. They derived their formulas from the conductance-precipitation values of Vickerey et al. (1981). In fact, the former is a direct follow-on paper to the latter, using a slightly different functional form and also rewriting the conductance relationships in terms of average energy rather than Maxwellian distribution characteristic energy.

The Vickerey et al. (1981) study used three days of incoherent scatter radar observations from Chatanika, Alaska, which they describe as quiet winter, active winter, and equinoctal conditions. Specifically, these days are 13 November 1976, 17 December 1976, and 6 April 1977. The figure from Vickerey et al. (1981) of the activity levels during these days is reproduced here in Figure 1, presenting the H component magnetic perturbations observed at the

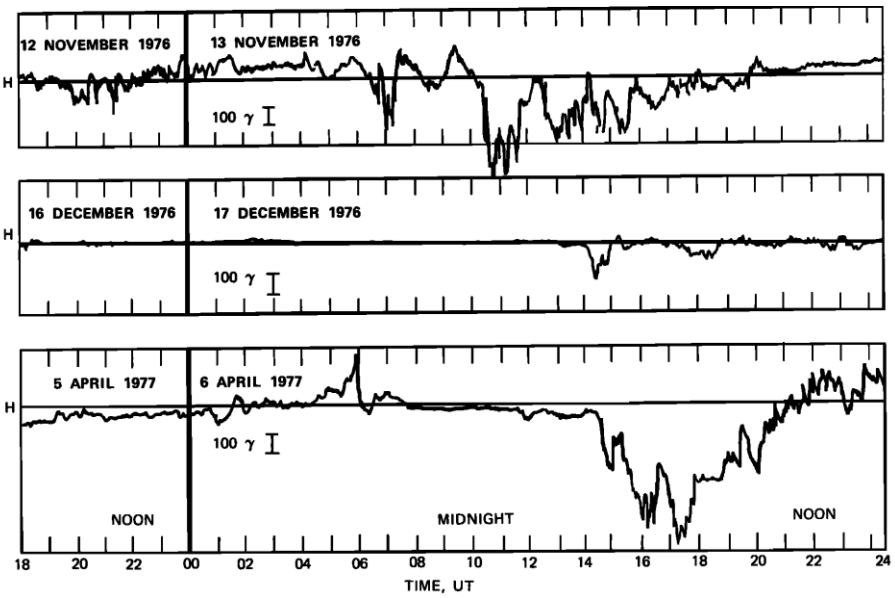

Figure 1. H component magnetograms for the three days of study from Vickerey et al. (1981). The local time of the measurements are indicated by the midnight and noon designations in the lower panel.

nearby College magnetometer station. From these values, local K indices were calculated, ranging from 0 to 7. The global-scale Dst and Kp indices during these three days had peak values of -105 nT and 7, respectively, occurring late on 6 April 1977. Unfortunately, the Chatanika radar was on the dayside during this time. The peak Dst and Kp values while the radar was observing a dark ionosphere were -43 nT and 5, respectively. While the auroral zone ranged from quiet to active during these three days, the extent of geomagnetic activity rose only up to the weak storm category (cf., Gonzalez et al., 1994)

The radar measurements provide the local electron density and temperature values along the beam path, from which a height-integrated conductance can be computed. Vickerey et al. (1981) then iteratively used the electron transport model of Rees (1963) to fit each observed density and temperature altitude profile with a modeled profile, thus yielding the primary beam characteristics of energy flux and average energy.

The Rees (1963) model assumes a precipitating beam of energetic electrons and performs the field-aligned transport and loss calculations for these particles. The resulting ionization values are then converted to density and temperature assuming local equilibrium chemical balance. The energetic electron transport component of the calculation is based on laboratory experiments of electron beam interactions with rarefied air, determining an ionization rate as a function of normalized "atmospheric depth." That is, it is essentially a stopping-power relationship for the primary electron precipitation beam, but because it is based on measurements from laboratory experiments, any ionization due to the production of secondary or tertiary electrons is also included in this relationship. Vondrak and Robinson (1985) validated the use of the Rees (1963) model for this purpose by using three passes of Atmospheric Explorer C (AE-C) electron precipitation measurements above the Chatanika radar observations, showing excellent agreement between the observed and derived electron densities.

The resulting relationship of both Pedersen conductance and the Pedersen-to-Hall conductance ratio are shown in Figure 2 (from Robinson et al., 1987). The figure shows a comparison of the Robinson formulas with those from Vickerey et al. (1981), based on the same data but with a slightly different functional form, and two other studies of this relationship. Spiro

et al. (1982) conducted a large-scale statistical compilation of energetic electron precipitation from AE-C data and then used the Vondrak and Baron (1976) numerical model to convert these values into ionization rates and eventually ionospheric conductance values. The other values in Figure 2 are from Wallis and Budzinski (1981), who did a similar procedure with a statistical compilation of electron precipitation data from Isis 2, then using the Rees (1963) model to obtain conductances. While all values are within a factor of three for any given average energy, that translates into a significant difference in terms of ionospheric response to magnetospheric driving. In addition, no error bars are given to understand the uncertainty surrounding these values.

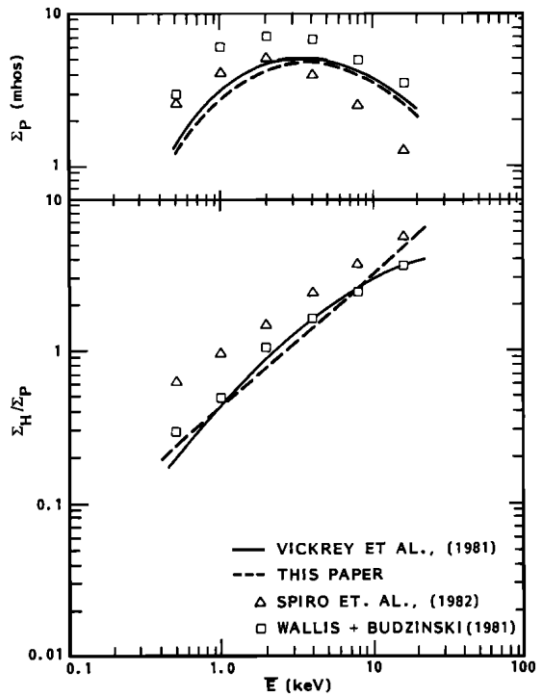

Figure 2. Relationships of conductance to average energy from Robinson et al. (1987). The top panel shows Pedersen conductance and the lower panel shows the Pedersen to Hall ratio. Values from several other studies are also shown.

The technique section of both the Vickerey et al. (1981) and Robinson et al. (1987) papers are quite short. Neither paper provides much detail about the numerical calculations, relying on the cited literature. More importantly, neither paper provides any information about the fitting routine used to obtain the final functional forms and coefficients, or any metrics assessment in creating these formulas.

To distill this somewhat convoluted path to the Robinson conductance formulas, they are derived from three days of radar measurements during relatively quiet to moderate activity, with the precipitating flux values coming not from satellite observations but from a simple ionization model based on laboratory electron beam experiments, with no discussion of how the iterative fitting method was conducted. While a side study showed that the ionization values from this model are very good, that also was based on a very limited data set of only three satellite passes over the radar station. As Welling et al. (2017) have argued, this limited activity level and data set inclusion leading to the Robinson formulas limits the applicability of these formulas. Many studies examine storm times well beyond the range of inputs used to create the Robinson formulas, which means those newer studies are extrapolating the usage of the Robinson formulas beyond their range of validity.

3. Alternatives to the Robinson formulas

Since the publication of Robinson et al. (1987), there has been significant effort towards improving our understanding of the precipitation-conductance relationship. This has come in the form of new statistical compilations of precipitation and ionospheric data as well as new numerical approaches to energetic electron transport. Below are a few highlights of these developments.

Several studies have created conductance parameterizations with new observational analysis. For example, ionospheric conductance has been related to field-aligned currents, as was done by Ridley & Liemohn (2002) and Ridley et al. (2004), using ground-based magnetometer data from January 1997 in the AMIE model. Cosgrove et al. (2009) examined Sondrestrom incoherent scatter radar data for a 40 hour interval in 1997, one that included a moderate storm. They then used the AMIE procedure to obtain gridded conductance values from these measurements. They found that spatial resolution is critical when determining Joule heating from ionospheric electrodynamics results; there are sub-grid electric field features as well as an overestimation of Joule heating if the large-scale electric field is too large. Cousins et al. (2015) created a conductance model of empirical orthogonal functions (EOFs) by combining observations from the Super Dual Auroral Radar Network (SuperDARN) and the Active Magnetosphere and Planetary Electrodynamics Response Experiment (AMPERE) satellite constellation. They included two different settings of a background offset value for the conductance, in addition to the FAC-driven conductance settings, a technique similar to Ridley et al. (2004). In a direct follow-on to Ridley et al. (2004), Mukhopadhyay et al. (2020) modified the methodology and expanded the data set to a full year of AMIE results – all of 2003, which included several superstorms – to create a model of the FAC-conductance relationship applicable to extreme event conditions. Another relationship between FACs and conductance has been created by Robinson et al. (2020), who used 9 storm days of Poker Flat Incoherent Scatter Radar (PFISR) observations with AMPERE derived FACs.

Kaeppler et al. (2015) followed the same methodology as that behind the Robinson formulas, producing a corrected version of them. They used incoherent scatter rader data from three substorm intervals of ~3 h each to obtain a compilation of conductance values and then iteratively used the Global Airglow (GLOW) two-stream electron transport model to obtain electron precipitation characteristics. They provide an excellent description of their methodology, including the iterative fitting procedure and present an initial usage of these new relationships. The study suffers from the same issue as the original Robinson formulas, though, in that it is based on a very limited data set of only a few active-time intervals.

McGranaghan et al. (2016) produced an EOF mapping of ionospheric conductance similar to Cousins et al. (2015), this time based on Defense Meteorological Satellite Program (DMSP) electron precipitation measurements instead of FACs. They used many years of DMSP electron flux data, then running the GLOW model to obtain ionospheric parameters for a calculation of conductance. They separated the influence of discrete and diffuse precipitation and, like others, included a background offset value. While this study provides high-latitude maps of conductance as a function of driving conditions, it was obtained without the use of direct measurements of ionospheric parameters.

Another study to mention is that of Knight et al. (2018), who combined ultraviolet images of the aurora from the Thermosphere-Ionosphere-Mesosphere Energetics and Dynamics (TIMED) spacecraft with ground-based ionosonde measurements to examine E-region dynamics. While not explicitly calculating height-integrated conductance, the findings of this study have implications for conductance relationships. In particular, their newly-obtained scaling associations between ionogram data and ionospheric density could help with the incorporation of such observations into precipitation-conductance relationships.

There have also been many numerical models of electron auroral zone transport since the creation of the Robinson formulas, any one of which could be used to rederive the precipitation-

conductance relationship. One of the more famous models developed in this timeframe is the GLOW model of Solomon et al. (1988), a two-stream transport code with the added features of airglow and auroral emission calculation for many electronic transitions. Similarly, the well-known field-line interhemispheric plasma (FLIP) model came into existence around this time (Newberry et al., 1989), a code that merged a two-stream energetic electron transport model with the chemistry and transport of the thermal plasma properties. Other codes focused solely on the energetic electrons, such as the Lummerzheim et al. (1992) multistream electron precipitation model and the Feautrier method code of Link (1992). The Khazanov & Liemohn (1995) model was also a multistream model and was one of the first to introduce a non-uniform magnetic field into the calculation, allowing for studies of the scattering from the pitch angle domain trapped zone to the loss cone.

A few studies have explored the relationship of precipitation to altitude-dependent ionization rates. Frahm et al. (1997) used the Link model to develop such profiles, and Fang et al. (2010) used the Lummerzheim model for a similar purpose. One study, Khazanov et al. (2018), went further than this, using the Khazanov & Liemohn model to compute Pedersen and Hall conductances and relate these to the Robinson formulas. Yu et al. (2018) used the GLOW model instead of the Robinson formulas within a coupled global geospace simulation, demonstrating that the Robinson formulas are perhaps not even needed for large-scale modeling efforts.

4. A possible numerical fix to the Robinson formulas

Khazanov et al. (2018) argued that numerical models that use the Robinson formulas with model-derived precipitation fluxes are underestimating the true conductance because the modeled precipitation does not take into account secondary electron production or transport of either the primary or secondary electrons out of the ionosphere back into the magnetosphere. They further postulated that these upflowing electrons would, for the most part, traverse the magnetospheric portion of the field line and augment the primary precipitation in the conjugate hemisphere. They continued the reasoning that electrons should leave the conjugate ionosphere, fly through the magnetosphere along the field line, and join the original primary precipitation into the first ionosphere. This should continue until the solution converges, creating a multiplicative effect on the originally precipitating electron spectrum. Khazanov et al. (2018) show calculated augmentation factors of ~3 near the peak of the primary precipitation energy spectrum and up to ~100 in the lower energy portion of the primary spectrum. It also mentioned an atmospheric backscatter rate of 15-40% for electrons in the primary precipitation energy range. From these larger, converged (after multiple reflections) electron flux values, they calculated ionization rates and eventually conductance values, resulting in a correction factor for the Robinson formulas. These correction factors are between 1.3 to 2.3, increasing with the characteristic energy of the initially precipitating electrons. Building on the Chen et al. (2019) modeling results, these correction factors have been used by Khazanov et al. (2019) within a kinetic drift physics approach, showing enhanced injection into the inner magnetosphere due to the higher conductance in the mid-latitude nightside region.

While the Khazanov et al. (2018) correction to the Robinson formulas appears to be a reasonable approach, there are several problems with the calculation. The main issue is an inconsistency between the backscatter rates and the eventual converged flux values. With each successive reflection of the electrons, the flux increases, not only the downward flux but also the

upward flux, each in an infinite series, which is convergent when $r < 1$, which is the case for reflected fluxes:

$$\phi_{down} = \phi_i \sum_{i=0}^{\infty} r^{-i} = \frac{\phi_i}{1-r} \quad (3)$$

$$\phi_{up} = r\phi_i \sum_{i=0}^{\infty} r^{-i} = \frac{r\phi_i}{1-r} \quad (4)$$

Here ϕ_i is the initial downward flux at some energy before any reflection and r is the reflection coefficient, $\phi_{up} = r\phi_{down}$, assuming identical reflection in each hemisphere.

Note that the relationship between the converged downward and upward fluxes in (3) and (4) shows that $\phi_{down} - \phi_{up} = \phi_i$ and that the ratio of downward to upward converged flux is $1/r$.

To achieve a converged downward flux that is three times higher than the initial downward flux, the lower bound of flux increase due to multiple reflection as found by Khazanov et al. (2018), r must be 0.67. The converged upward flux should then be only 33% smaller than the converged downward flux. To achieve a converged flux 100 times larger than the initial primary precipitation, r needs to be 0.99 and the converged upward flux will be nearly identical to the converged downward flux. This is inconsistent with the backscatter ratios stated in Khazanov et al. (2018) of 15-40%. These r values yield converged downward fluxes of only 1.2 to 1.7 times the initial precipitating flux without reflection. These two sets of numbers, the low backscatter rates and the large flux increase from multiple reflection, are incompatible.

The parity of the fluxes should be observable by both low-Earth-orbit spacecraft as well as satellites near the magnetic equatorial region. At low altitudes, The Fast Auroral SnapshoT (FAST) spacecraft provides an excellent data set for considering this question. For example, the study of Dombeck et al. (2018) directly addresses this issue with the case studies they present. Figure 3a is a reproduction of their Figure 6, showing an illustrative example of the velocity space distribution of electron energy flux for nightside auroral-zone non-accelerated precipitation (i.e., the diffuse aurora). Figure 3b is their Figure 5, showing the field-aligned differential energy flux in the upward and downward directions, along with the ratio between these two quantities.

Figure 3 reveals a truth from the Khazanov et al. (2018) study: there are indeed upward-flowing electrons at all energies within the diffuse aurora. In fact, the plots show that the upward secondary electrons below 100 eV have a larger flux than the downward flux at these energies, consistent with the modeling of Khazanov et al. (2018), and much older modeling results, such as Evans (1974). At higher energies, in particular above the 500 eV cutoff used by Khazanov et al. (2018) to define the primary precipitation beam, the upward flux is quite depleted relative to the downward flux.

The ratio, between 2 and 10 in the cyan dots of Figure 3b, is fairly consistent with the 15% - 40% backscatter rate of the primary beam mentioned in Khazanov et al. (2018). That is, electrons are indeed leaving the upper atmosphere and the observed ratio between the incoming and outgoing fluxes are consistent with modeling. Again, this is fully consistent with the modeling work of Evans (1974), who also found that the primary beam electrons had a 40% or lower backscatter rate. To be clear: these observations are consistent with the backscatter rates but not the flux multiplication factors from Khazanov et al. (2018).

In the plasma sheet, where strong pitch angle scattering can be assumed to dominate (e.g., Chen & Schulz, 2001; Thorne et al., 2010), the loss cone is filled by wave-particle interactions on time scales faster than a bounce period. Any secondary or backscattered population coming out of the ionosphere will experience this same pitch angle scattering at the same fast rate as the primary particle population. That is, regardless of the upgoing flux, if the loss cone is being filled due to scattering in the plasma sheet, then the upgoing flux of reflected and backscattered particles should isotropize with the trapped magnetospheric population due to that same scattering process. Data clearly supports a single backscatter but refutes multiple reflection..

(a) Velocity space distribution of wave-scattered precipitation

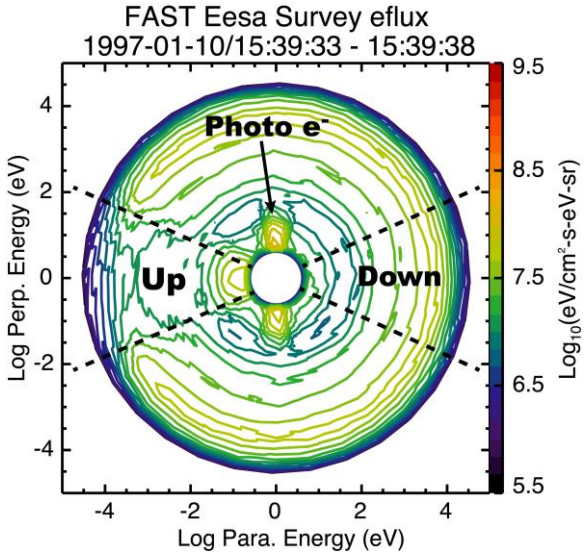

(b) Differential energy flux along the upward and downward field-aligned directions

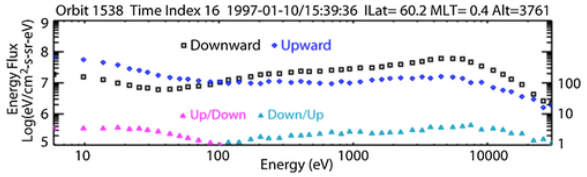

Figure 3. Reproduced from Dombeck et al. (2018), (a) a plot of the diffuse auroral electron energy flux velocity space distribution. The population marked "photo e-" are spacecraft photoelectrons, and the "Up" and "Down" regions within the dashed lines denote the pitch angles connected to the thermosphere. (b) The upward and downward fluxes for that same time, and the ratio between them in pink and cyan, along the bottom and using the scale on the right.

How can it be that Khazanov et al (2018) compute backscatter values consistent with observations but inconsistent downward-to-upward flux ratios? The explanation could be in the implementation of precipitation within the code. In the modeling study of Khazanov et al. (2018), it could be that the initial primary electron flux (at energies above 500 eV) is continuously added to the electron distribution in the loss cone, perhaps at the top of the ionosphere at 800 km altitude. Following a particular packet of particles through a full bounce period, it would then gain the initial distribution every half-bounce period (as the packet crosses the 800 km altitude region in the downward direction in each hemisphere). The flux can then build up with each successive bounce. Without collisions and loss, it would build up to an infinite value, but the particles experience these processes along the field line, especially below

800 km in the upper atmosphere and ionosphere. The fluxes in these model calculations would then build up until equilibrium is reached; when the scattering and loss along half a bounce is equal to the initial spectrum flux values being added to the solution on that cadence. This could be what is leading to an erroneously high flux in the multiple-reflection scenario (by a factor of 3 to 100) discussed by Khazanov et al. (2018).

5. Conclusions and a Call to Action

The Robinson formulas have been a tremendous asset to the space physics community. The availability of a straightforward relationship between precipitating electron parameters and the resulting ionospheric Pedersen and Hall conductances has been highly valuable for advancing knowledge of geospace. Its inclusion in regional and global modeling studies has allowed scholars to assess the nonlinear dynamics of the magnetosphere-ionosphere system, proving to be a simple yet powerful tool for new understanding.

For all of their ubiquitous usage across space physics, however, the Robinson formulas are in need of an update. They are based on a small data set using a simplistic model without much detail on the iterative process used to obtain the fit. They do not represent the state of the art in scientific methodology, and more robust relationships could be devised. It is suggested as an action item to the community to develop a next-generation precipitation-to-conductance relationship.

Perhaps the biggest concern with the Robinson formulas is that they are based on only three days of incoherent radar data of moderate activity, which means that any usage of them for intense storm times is an extrapolation of their range of validity. Welling et al. (2017) argued that this small activity ranges in underlying and embedded codes within global modeling frameworks bring into question the usage of the coupled global model for intense storm intervals. This is a big problem for advancing space physics knowledge as well as for advancing space weather forecasting capabilities (e.g., Opgenoorth et al., 2019; Morley, 2020).

With the advent of the advanced modular incoherent scatter radar facilities, ground based measurements of the ionospheric parameters in the conductivity equations are widely available. Furthermore, the continued availability of energetic particle precipitation data, such as from FAST, the newly calibrated values from DMSP (Redmon et al., 2017), and several other low-Earth-orbiting spacecraft, are critically important for this task. Some studies have also started performing these statistical compilations. It is proposed that a valuable step forward is a combination of the Kaeppler et al. (2015) and McGranaghan et al. (2016) approaches, using a large database of simultaneously measured electron precipitation flux and ionospheric characteristics. The direct linkage of these two data sets removes the need for an electron transport calculation to provide one or the other of these quantities.

Better modeling relationships between electron precipitation and ionization profiles exist, but we need to incorporate and assess these models against observations within local, regional, and global modeling scenarios. The general approach of the Khazanov et al. (2018) study, using a sophisticated numerical model to create a better relationship between precipitation and conductance, is highly appropriate for making progress on this topic. We should not only correct the Robinson formulas, but conduct the relational study again, with the large observational sets providing a counterweight to the many numerical approaches available for such a leap forward. Combining data and modeling with robust metrics applications, as discussed recently by Morley

et al. (2018), Liemohn et al. (2018), and Zheng et al. (2019), for example, will allow a full assessment of the strengths and limitations of such a model.

Others in the community have already been making the call for new studies on ionospheric conductance. Several reports of community effort have included this request to improve our understanding of conductance. For example, Yu et al. (2019) stated that "it is necessary to capture the mutually consistent electric field and magnetospheric configuration." The magnitude and spatial pattern of the ionospheric conductance is a vital component of this mutual dependence. Robinson et al. (2019) discussed the impact of ionospheric conductance on various space weather phenomena as well as metrics requirements for a robust data-model comparison of this quantity. Very recently, Öztürk et al. (2020) listed the main components of the ongoing Ionospheric Conductance Challenge across the research community. The three pillars of this effort include quantifying the uncertainties within existing conductance models, performing simulations of available global models with identical inputs to assess the influence of conductance on the geospace system, and the creation of better conductance models. The call to action from this Commentary is more specific, focusing attention on one critical link in the conductance calculation – its relationship to energetic electron precipitation.

Acknowledgments

This work was supported by NASA grants NNX17AB87G and 80NSSC17K0015 and NSF grant 1663770. There is no new data for this article; all figures are reused with permission.

References

Brambles, O. J., Lotko, W., Zhang, B., Wiltberger, M., Lyon, J., & Strangeway, R. J. (2011). Magnetosphere Sawtooth Oscillations Induced by Ionospheric Outflow. *Science*, *332*, 1183-1186. https://doi.org/10.1126/science.1202869

Chen, M. W., & Schulz, M. (2001). Simulations of storm time diffuse aurora with plasmasheet electrons in strong pitch angle diffusion, *Journal of Geophysical Research, 106,* 1873–1886.

Chen, M. W., Lemon, C. L., Hecht, J., Sazykin, S., Wolf, R. A., Boyd, A., & Valek, P. (2019). Diffuse auroral electron and ion precipitation effects on RCM-E comparisons with satellite data during the 17 March 2013 storm. *Journal of Geophysical Research: Space Physics*, 124, 4194– 4216. https://doi.org/10.1029/2019JA026545

Cosgrove, R. B., Lu, G., Bahcivan, H., Matsuo, T., Heinselman, C. J., & McCready, M. A. (2009). Comparison of AMIE-modeled and Sondrestrom-measured Joule heating: A study in model resolution and electric field–conductivity correlation. *Journal of Geophysical Research, 114,* A04316. https://doi.org/10.1029/2008JA013508

Cousins, E. D. P., Matsuo, T., & Richmond, A. D. (2015), Mapping high-latitude ionospheric electrodynamics with SuperDARN and AMPERE, *Journal of Geophysical Research Space Physics, 120,* 5854– 5870, doi:10.1002/2014JA020463.

444 Dombeck, J., Cattell, C., Prasad, N., Meeker, E., Hanson, E., & McFadden, J. (2018).
445 Identification of auroral electron precipitation mechanism combinations and their
446 relationships to net downgoing energy and number flux. *Journal of Geophysical*
447 *Research: Space Physics, 123*, 10,064–10,089. https://doi.org/10.1029/2018JA025749

448 Evans, D. S. (1974). Precipitating electron fluxes formed by a magnetic field aligned potential
449 difference. *Journal of Geophysical Research, 79*, 2853– 2858.
450 https://doi.org/10.1029/JA079i019p02853

451 Fang, X., Randall, C. E., Lummerzheim, D., Wang, W., Lu, G., Solomon, S. C., & Frahm, R. A.
452 (2010). Parameterization of monoenergetic electron impact ionization. *Geophysical*
453 *Research Letters*, *37*, L22106. doi:10.1029/2010GL045406.

454 Fedder, J. A., Slinker, S. P., Lyon, J. G., & Elphinstone, R. D. (1995). Global numerical
455 simulation of the growth phase and the expansion onset for a substorm observed by
456 Viking. *Journal of Geophysical Research, 100*(A10), 19083– 19093,
457 doi:10.1029/95JA01524.

458 Frahm, R. A., Winningham, J. D., Sharber, J. R., Link, R., Crowley, G., Gaines, E. E., Chenette,
459 D. L., Anderson, B. J., & Potemra, T. A. (1997). The diffuse aurora: A significant source
460 of ionization in the middle atmosphere. *Journal of Geophysical Research, 102*, 28,203.
461 https://doi.org/10.1029/97JD02430

462 Gonzalez, W. D., Joselyn, J. A., Kamide, Y., Kroehl, H. W., Rostoker, G., Tsurutani, B. T., &
463 Vasyliunas, V. M. (1994). What is a geomagnetic storm? *Journal of Geophysical*
464 *Research, 99*(A4), 5771– 5792, doi:10.1029/93JA02867.

465 Kaeppler, S. R., Hampton, D. L., Nicolls, M. J., Strömme, A., Solomon, S. C., Hecht, J. H., &
466 Conde, M. G. (2015). An investigation comparing ground-based techniques that quantify
467 auroral electron flux and conductance, *Journal of Geophysical Research Space Physics,*
468 *120, 9038–9056*, https://do.org/10.1002/2015JA021396

469 Khazanov, G. V., & Liemohn, M. W. (1995). Nonsteady state ionosphere-plasmasphere coupling
470 of superthermal electrons. *Journal of Geophysical Research, 100*, 9669.

471 Khazanov, G. V., Robinson, R. M., Zesta, E., Sibeck, D. G., Chu, M., & Grubbs, G. A. (2018).
472 Impact of precipitating electrons and magnetosphere-ionosphere coupling processes on
473 ionospheric conductance. *Space Weather, 16*, 829–837.
474 https://doi.org/10.1029/2018SW001837

475 Khazanov, G. V., Chen, M. W., Lemon, C. L., & Sibeck, D. G. (2019). The magnetosphere-
476 ionosphere electron precipitation dynamics and their geospace consequences during the
477 17 March 2013 storm. *Journal of Geophysical Research: Space Physics, 124*, 6504–
478 6523. https://doi.org/10.1029/2019JA026589

479 Knight, H. K., Galkin, I. A., Reinisch, B. W., & Zhang, Y. (2018). Auroral ionospheric *E* region
480 parameters obtained from satellite-based far ultraviolet and ground-based ionosonde
481 observations: Data, methods, and comparisons. *Journal of Geophysical Research: Space*
482 *Physics, 123*, 6065– 6089. https://doi.org/10.1029/2017JA024822

483 Liemohn, M. W., Ridley, A. J., Brandt, P. C., Gallagher, D. L., Kozyra, J. U., Mitchell, D. G.,
484 Roelof, E. C., & DeMajistre, R. (2005). Parametric analysis of nightside conductance

effects on inner magnetospheric dynamics for the 17 April 2002 storm. *Journal of Geophysical Research, 110,* A12S22. https://doi.org/10.1029/2005JA011109.

Liemohn, M. W., McCollough, J. P., Jordanova, V. K., Ngwira, C. M., Morley, S. K., Cid, C., Tobiska, W. K., Wintoft, P., Ganushkina, N. Y., Welling, D. T., Bingham, S., Balikhin, M. A., Opgenoorth, H. J., Engel, M. A., Weigel, R. S., Singer, H. J., Buresova, D., Bruinsma, S., Zhelavskaya, I., Shprits, Y. Y., & Vasile, R. (2018). Model evaluation guidelines for geomagnetic index predictions. *Space Weather*, *16*, 2079– 2102. https://doi.org/10.1029/2018SW002067

Link, R. (1992). Feautrier solution of the electron transport equation. *Journal of Geophysical Research*, *97,* 159.

Lummerzheim, D., Rees, M. N. & Anderson, H. R. (1989). Angular dependent transport of auroral electrons in the upper atmosphere. *Planetary and Space Science*, *37*, 109.

McGranaghan, R., Knipp, D. J., Matsuo, T., & Cousins, E. (2016). Optimal interpolation analysis of high-latitude ionospheric Hall and Pedersen conductivities: Application to assimilative ionospheric electrodynamics reconstruction. *Journal of Geophysical Research: Space Physics*, *121*, 4898–4923. https://doi.org/10.1002/2016JA022486

Morley, S. K. (2020). Challenges and opportunities in magnetospheric space weather prediction. *Space Weather*, *18*, e2018SW002108. https://doi.org/10.1029/2018SW002108

Morley, S. K., Brito, T. V., & Welling, D. T. (2018). Measures of model performance based on the log accuracy ratio. *Space Weather*, *16*, 69–88. https://doi.org/10.1002/2017SW001669

Mukhopadhyay, A., Welling, D. T., Liemohn, M. W., Ridley, A. J., Chakraborty, S., & Anderson, B. J. (2020). Conductance model for extreme events: Impact of auroral conductance on space weather forecasts. *Space Weather*, submitted, manuscript # 2020SW002551. https://www.essoar.org/doi/abs/10.1002/essoar.10503207.1

Newberry, I. T., Comfort, R. H., Richards, P. G., & Chappell, C. R. (1989). Thermal He+ in the plasmasphere: Comparison of observations with numerical calculations. *Journal of Geophysical Research*, *94*, 15265.

Opgenoorth, H. J., Wimmer-Schweingruber, R. F., Belehaki, A., Berghmans, D., Hapgood, M., Hesse, M., Kauristie, K., Lester, M., Lilensten, J., Messerotti, M., & Temmer, M. (2019). Assessment and recommendations for a consolidated European approach to space weather – as part of a global space weather effort. *Journal of Space Weather and Space Climate*, *9*, A37, DOI: 10.1051/swsc/2019033

Öztürk, D. S., Garcia-Sage, K., & Connor, H. K. (2020). All hands on deck for ionospheric modeling. *Eos*, *101*, https://doi.org/10.1029/2020EO144365.

Perlongo, N., Ridley, A., Liemohn, M. W., & Katus, R. M. (2017), The effect of ring current electron scattering rates on magnetosphere-ionosphere coupling. *Journal of Geophysical Research*, *122*, 4168-4189, doi:10/1002/2016JA023679

Redmon, R. J., Denig, W. F., Kilcommons, L. M., & Knipp, D. J. (2017). New DMSP database of precipitating auroral electrons and ions. *Journal of Geophysical Research Space Physics*, *122*, 9056–9067, doi:10.1002/2016JA023339.

Rees, M. H. (1963). Auroral ionization and excitation by incident energetic electrons. *Planetary and Space Science, 11*, 1209, 1963.

Ridley, A. J., & Liemohn, M. W. (2002). A model-derived storm-time asymmetric ring current driven electric field description, *Journal of Geophysical Research, 107*(A8), 1151. https://doi.org/10.1029/2001JA000051

Ridley, A. J., Gombosi, T. I., & De Zeeuw, D. L. (2004). Ionospheric control of the magnetosphere: Conductance. *Annales Geophysicae, 22*, 567.

Robinson, R. M., Vondrak, R. R., Miller, K., Dabbs, T., & Hardy, D. (1987). On calculating ionospheric conductances from the flux and energy of precipitating electrons. *Journal of Geophysical Research, 92*, 2565. https://doi.org/10.1029/JA092iA03p02565

Robinson, R., Zhang, Y., Garcia-Sage, K., Fang, X., Verkhoglyadova, O. P., Ngwira, C., et al. (2019). Space weather modeling capabilities assessment:Auroral precipitation and high-latitude ionospheric electrodynamics. *Space Weather, 17*, 212–215. https://doi.org/10.1029/2018SW002127

Robinson, R. M., Kaeppler, S. R., Zanetti, L., Anderson, B., Vines, S. K., Korth, H., & Fitzmaurice, A. (2020). Statistical relations between auroral electrical conductances and field-aligned currents at high latitudes. *Journal of Geophysical Research: Space Physics*, 125, e2020JA028008. https://doi.org/10.1029/2020JA028008

Solomon, S. C., Hays, P. B., & Abreu, V. J. (1988). The auroral 6300 Å emission: Observations and modeling. *Journal of Geophysical Research, 93*, 9867, 1988.

Spiro, R. W., Reiff, P. H., & Maher, L. J. (1982). Precipitating electron energy flux and auroral zone conductances-An empirical model. *Journal of Geophysical Research, 87*(A10), 8215– 8227, doi:10.1029/JA087iA10p08215.

Thorne, R. M., Ni, B., Tao, X., Horne, R. B., & Meredith, N. P. (2010). Scattering by chorus waves as the dominant cause of diffuse auroral precipitation. *Nature, 467*(7318), 943–946. https://doi.org/10.1038/nature09467

Vickerey, J. F., Vondrak, R. R., & Matthews, S. J. (1981). The diurnal and latitudinal variations of auroral zone ionospheric conductivity. *Journal of Geophysical Research, 86*, 65.

Vondrak, R. R., & Baron, M. J. (1976). Radar measurements of the latitudinal variation of auroral ionization. *Radio Science, 11*(11), 939– 946, doi:10.1029/RS011i011p00939.

Vondrak, R., & Robinson, R. (1985). Inference of high-latitude ionization and conductivity from AE-C measurements of auroral electron fluxes. *Journal of Geophysical Research, 90*, 7505, 1985.

Wallis, D. D., & Budzinski, E. E. (1981). Empirical models of height integrated conductivities. *Journal of Geophysical Research, 86*(A1), 125– 137, doi:10.1029/JA086iA01p00125.

Welling, D. T., Anderson, B. J., Crowley, G., Pulkkinen, A. A., & Rastätter, L. (2017). Exploring predictive performance: A reanalysis of the geospace model transition challenge. *Space Weather, 15*, 192–203, doi:10.1002/2016SW001505.

Wiltberger, M., Rigler, E. J., Merkin, V., & Lyon, J. G. (2017). Structure of high latitude currents in magnetosphere-ionosphere models. *Space Science Reviews*, *206*, 575. https://doi.org/10.1007/s11214-016-0271-2

Yu, Y., Jordanova, V. K., Ridley, A. J., Albert, J. M., Horne, R. B., & Jeffery, C. A. (2016). A new ionospheric electron precipitation module coupled with RAM-SCB within the geospace general circulation model. *Journal of Geophysical Research: Space Physics*, *121*, 8554–8575. https://doi.org/10.1002/2016JA022585

Yu, Y., Jordanova, V. K., McGranaghan, R. M., & Solomon, S. C. (2018). Self-consistent modeling of electron precipitation and responses in the ionosphere: Application to low-altitude energization during substorms. *Geophysical Research Letters*, *45*, 6371– 6381. https://doi.org/10.1029/2018GL078828

Yu, Y., Liemohn, M. W., Jordanova, V. K., Lemon, C., & Zhang, J. (2019). Recent advancements and remaining challenges associated with inner magnetosphere cross-energy/population interactions (IMCEPI). *Journal of Geophysical Research: Space Physics*, *124*, 886– 897. https://doi.org/10.1029/2018JA026282

Zhang, B., Lotko, W., Brambles, O., Wiltberger, M. & Lyon, J. (2015). Electron precipitation models in global magnetosphere simulations. *Journal of Geophysical Research Space Physics*, *120*, 1035– 1056. doi: 10.1002/2014JA020615.

Zheng, Y., Ganushkina, N. Y., Jiggens, P., Jun, I., Meier, M., Minow, J. I., et al. (2019). Space radiation and plasma effects on satellites and aviation: Quantities and metrics for tracking performance of space weather environment models. *Space Weather*, *17*, 1384– 1403. https://doi.org/10.1029/2018SW002042

Figure 1.

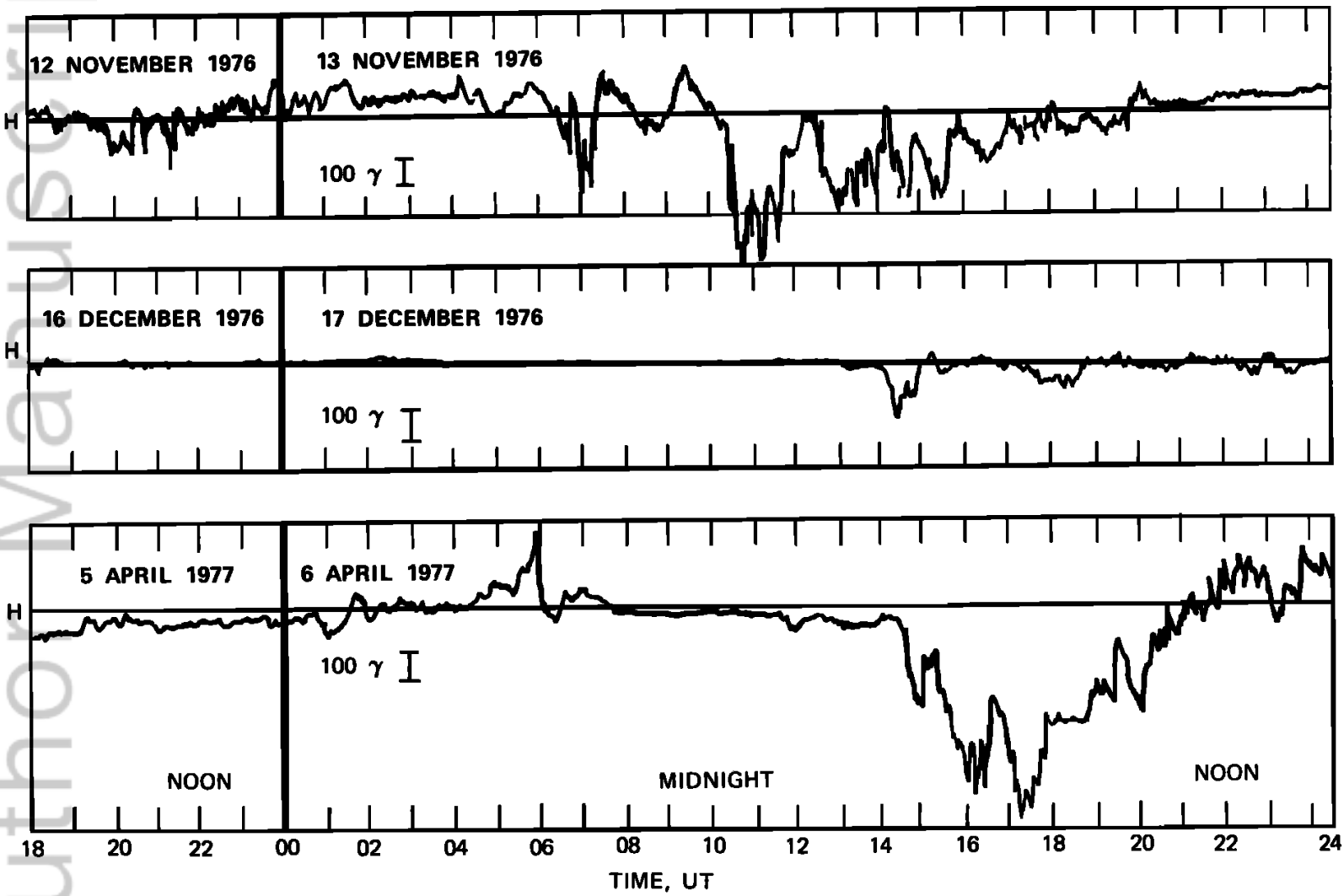

Figure 2.

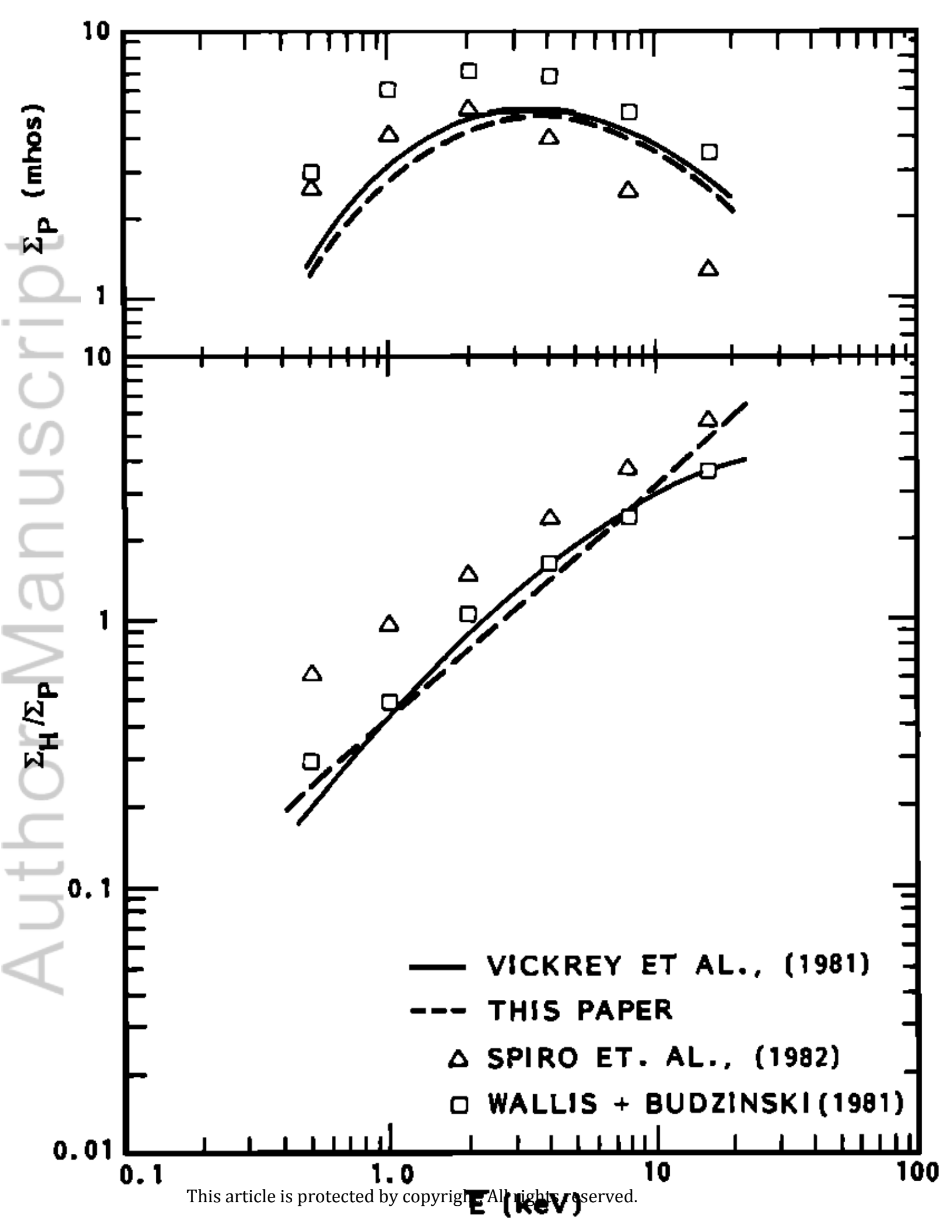

Figure 3.

(a) Velocity space distribution of wave-scattered precipitation

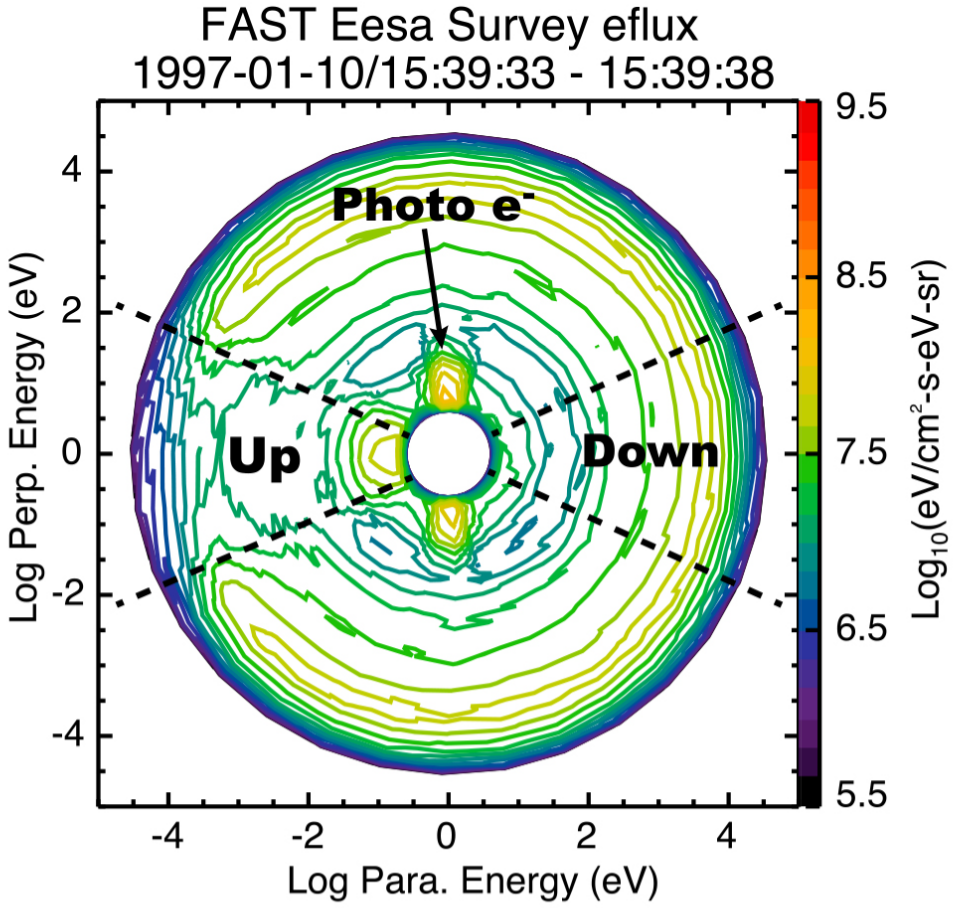

(b) Differential energy flux along the upward and downward field-aligned directions, and their ratio